Okojie *et al.*
Journal of Engineering and Applied Science (2022) 69:96
https://doi.org/10.1186/s44147-022-00146-9

Journal of Engineering and Applied Science

RESEARCH Open Access

Harmonic generation of variable speed drive under complex-voltage unbalance conditions

Daniel Esene Okojie[1*], Henry Ogbemudia Omoregbee[2], Coneth Graham Richards[1], Agha Francis Nnachi[1] and Bertus Wilhelm Bornebroek[1]

*Correspondence: OkojieDE@tut.ac.za

[1] Department of Electrical Engineering, Tshwane University of Technology, Emalahleni Campus, Mpumalanga, South Africa

[2] Mechanical Engineering Department, University of Lagos, Lagos, Nigeria

Abstract

Efficiency in the industrial sector is a priority when seeking to minimize production costs and reduction in losses. Harmonic generation and associated losses need to be treated carefully with broad implementation of variable speed induction motor applications. The effect of these induced losses can add up to a significant loss. This study uses statistical tools alongside synthesized models to deduce and compare outcomes from regulated and unregulated converters in which harmonics may be triggered by switching algorithm of modern switch-mode power supplies and other inductive loads attached to supply bus system. These harmonics accumulate over time due to losses propagating through connected equipment when changes occur on the bus system. In this regard, results obtained from investigating and comparing three original equipment manufacturer variable speed drives that were exposed to voltage unbalance and complex harmonic conditions are presented in this study. A conclusion accomplished from the investigation and comparison suggests that generation of 6-pulse uncontrolled rectifier losses is negligible. Experimental validation confirms that unregulated 6-pulse converter produces on average more harmonics compared to the regulated converter of standard as recommended in guideline to permissible harmonic tolerance.

Keywords: Original equipment manufacturer (OEM), Variable speed drives (VSD), Complex voltage unbalance, Total harmonic distortion (THD), Voltage source inverter (VSI), Current source inverter (CSI)

Introduction

Harmonics have been in power systems from the beginning of the creation of AC systems. It, however, has lately gained prominence as a result of the convergence of two trends: the rising concern of electric utilities to enhance power factor to avoid penalties, and the widespread use of power electronic equipment in modern industry seeking improved system dependability and efficiency. Varied harmonic frequencies with different amplitudes can be used to create a distorted periodic wave of any shape [1]. On the other hand, any distorted periodic wave can be decomposed into a fundamental and a collection of harmonic waves using Fourier analysis. The effects of non-linear elements in power systems can be thoroughly examined using this technique. Non-characteristic harmonics, also known as 'inter-harmonics,' are those that are not integer multiples of the fundamental power frequency. The cycloconverter is a key source of inter-harmonics. The term 'sub-harmonics' refers to a subset of inter-harmonics. Sub-harmonics are frequencies that are lower than the fundamental frequency.

The existing industrial process or manufacturing plant combines old and new technology to ensure advancement in technology and economic development of finished products. These combinations could lead to contamination of power quality through the additions of industrial electric bus systems. As concluded in "Harmonics and inter-harmonics in general VSI/CSI inverters: Analysis, modeling and simulation, observations of voltage, frequency, and harmonics were made in the form of practical loss factors [2]." The inclusion of these voltage and current distortions affects both the overall output of the bus system and the installed equipment. In practice, calculating harmonic content at clearly defined points has only recently become commercially feasible. However, the calculation is mainly for providing harmonic monitoring, as established in "Input current inter-harmonics of Variable-Speed Drives due to motor current imbalance [3]."

The effect of harmonics can be summed up in terms of economic operating costs, equipment depreciation and equipment efficiency. The economic operating cost is a situation where the equipment built is operated as economically as possible with direct replacements, improvements and or enhancements supported by regular maintenance and cyclical resources. In order to track the installed equipment, some form of trend-based monitoring of power quality indices must be used to measure overall equipment health [4]. Process-related upsets affect the maintenance schedule and results' in premature failure of the equipment. The resulting deterioration of the equipment directly affects the life of the equipment, shortening the effective life due to degradation of the inner portion. If the equipment does not perform as required, the deterioration then relates to financial loss [5]. Total harmonics distortion (THD) is a factor that is commonly used to determine the deviation of distorted waveforms from a sine wave, and it is stated in relation to the degree of distortions in both the current and voltage waveforms in the power network. Appropriate requirements refer to reasonable inclusive harmonic material as a total harmonic distortion (THD) percentile of 8% in both voltage and current waveforms [6]. The International Electro-technical Commission (IEC) 61,000–4-30 often base the standard on analysis encompassed by several other standards as set out in 2015 such as "Power quality measurement methods" and IEC Standards 61,000–4-7. In addition, "General guide on harmonics and inter-harmonics measurement and instrumentation for power supply systems and equipment are also connected thereto". This includes equivalent standards as the South African National Standards (SANS) (1816:2019) electricity supply—quality of supply and power quality monitoring instruments specification [7] as well as SANS (62,586–1:2018) of "Power quality measurement in power supply systems"—part 1 and part 2 [8].

Harmonics produced during normal operation are subject to losses in the distribution systems that are not taken into account by the production unit when operating the installed equipment [9]. The effects of the induced harmonics can be mitigated or the phenomenon can be removed by applying specialized active or passive filters to the system this can be done only if, prior to the actual mitigating solution being introduced the particular spectrum of harmonics has been identified [10]. Due to the sampling rate of the measuring instruments, the resulting collected data may not be reliable.

Without relation to the complex displacement angle, the maximum and average values for voltage and current quantities are noted. The key issue is the effects of the harmonics generated by the variable speed drive system supplying the induction motor when the system is subject to complex conditions of supply voltage imbalance [11–13].

The flyback converter is a power supply architecture that uses a mutually linked inductor to store energy when current flows through it and release it when the power is turned off. In terms of architecture and performance, flyback converters are comparable to booster converters. Depending on the minimum value of the inductor current in each cycle, flyback converter operation can be classified into two modes. The current in the inductor is never zero if the MOSFET goes from OFF to ON before the inductor is entirely exhausted. Continuous conduction mode is the name for this action (CCM). Alternatively, if OFF lasts long enough for the primary inductor to entirely discharge, the current in the inductor will be zero for a period of time. Although a diode rectifier flyback converter can be designed to work only in CCM under all load and line conditions, this is usually not cost effective. A big inductance value is required to maintain the CCM at light load and high line. A flyback transformer's size and cost are frequently increased as a result of this. At light load, most practical flyback converters prefer to operate in DCM [14, 15].

In "Harmonics in electrical power systems: Effects of new technologies" the author used the total demand distortion (TDD), total harmonic distortion from current flow (THDi) and THD tests to calculate the harmonic distortion according to the Institute of Electrical and Electronics Engineers (IEEE) limits [16]. Furthermore, the author noted that resonant circuit operation, which supports harmonic propagation through VSD subsystems, poses substantial multiplication of harmonics. Different topologies, namely the VSI and CSI operate differently depending on the implementation of the particular device. Thus, for the AC the VSI will work on the basis of the unique conduction patterns in the inverter in either continuous current mode (CCM) or discontinuous current mode (DCM). The 5th harmonic may have a resultant magnitude of 90% of the basic in DCM, which is in stark contrast to 20% of the CSI inverter magnitude. Hence, for observed harmonic generation via a VSD method, the choice of topology is important [17].

M. Rane, 2019 [18] in their paper emphasize on the effect of unbalance and harmonics on the operation of standalone MG; this they said could be as a result of reduced power transfer from DER to load and also as an error produced in phase locked loop (PLL) operation. They, therefore, propose a positive sequence component (PSC)-based and dynamic phasor (DP)-based compensation techniques to mitigate the effect of unbalanced source voltage condition (UbSVC). From the simulation done, it was obtained that 46% enhancement in power transferred from DER was observed in the case of PSC-based compensation in comparison to 44% in the case of DP based compensation along with load voltage compensation. In a different work where dragonfly optimization algorithm for extracting maximum power of grid-interfaced PV systems was put into used [19] to solve the among others the problem of partial shading which is most severe in grid-connected photovoltaic (PV) systems as it reduces the grid efficiency. To achieve maximum power, PV system was made to utilize the maximum power point-tracking (MPPT) algorithms. And also, they proposed a two-level converter system for optimizing the PV power before injecting the power into the grid network. The boost converter was also used to regulate the MPPT algorithm and to make the grid-tied PV system operate under non-uniform weather conditions they utilize a dragonfly optimization algorithm (DOA)-based MPPT was put forward and applied due to its ability to trace the global peak thereby leading to higher efficiency and shorter response time.

When evaluating losses due to harmonics, depending on the topology and measure of voltage or current, each measure represents a different facet. As shown in Table 1, the current distortion limits are specified in accordance with IEEE 519 (IEEE recommended practice and specifications for harmonic control in electric power systems) [20].

This study provides an experimental comparison between three similar VSD OEMs with the device subjected to various imbalance conditions in a semi-isolated system in terms of loss generation as an act to provide clear understanding to the effect of harmonics and their associated losses which needs to be treated carefully as related to variable speed induction motor. In this regards, the study provides an investigation of how synthesized models could produce from regulated and unregulated converters harmonics via the use of statistical tool. As indicated in the "Methods" section, the loss tests performed is the method used to assess the efficiency of the OEM and analysis of the performance. Thus, the "Model Mathematical Derivation" section contains mathematical derivation of the model. "Variable speed drive" section comprises discussion on the variable speed drive motor. The "Experimental setup" section gives the experimental work setup while in the "Simulation" section is the simulation and results. In the "Results and discussion" section, the experimental result is discussed while the "Conclusion" section is the conclusion.

Methods

The aim of this study is to provide an experimental comparison between three similar VSD OEMs with the device subjected to various unbalance conditions in a semi-isolated system in terms of loss generation. Figure 1 shows the block flow diagram of the proposed topology for the harmonic propagation. To accomplish this aim, a mathematical model of the VSD is designed, simulated, and analyzed on a VSD-driven induction motor system subjected to complex voltage unbalances as shown in Fig. 2. This setup is such that it relate different (OEM) based on commercially available hardware with the intent of observing similar behavior based on the same simulation

Table 1 IEEE practice and specification for harmonic control

Isc/I_L	3 < h < 11	11 < h < 17	17 < h < 23	17 < h < 35	35 < h < 50	TDD
h < 20	4.0	2.0	1.5	0.6	0.3	5.0
20 < h < 50	7.0	3.5	2.5	1.0	0.5	8.0
50 < h < 100	10.0	4.5	4.0	1.5	0.7	12.0
100 < 1000	12.0	5.5	5.0	2.0	1.0	15.0
h > 1000	15.0	7.0	6.0	2.5	1.4	20.0

where *h* = harmonic number

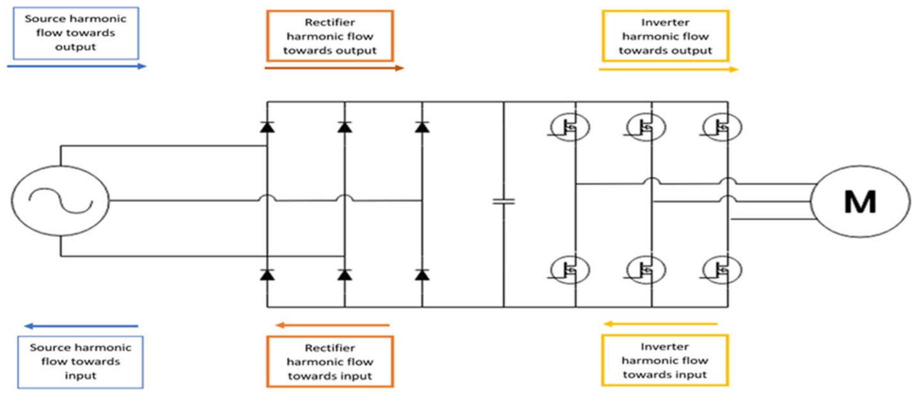

Fig. 1 Flowchart of the proposed topology of the harmonic propagation through VSD sub-system

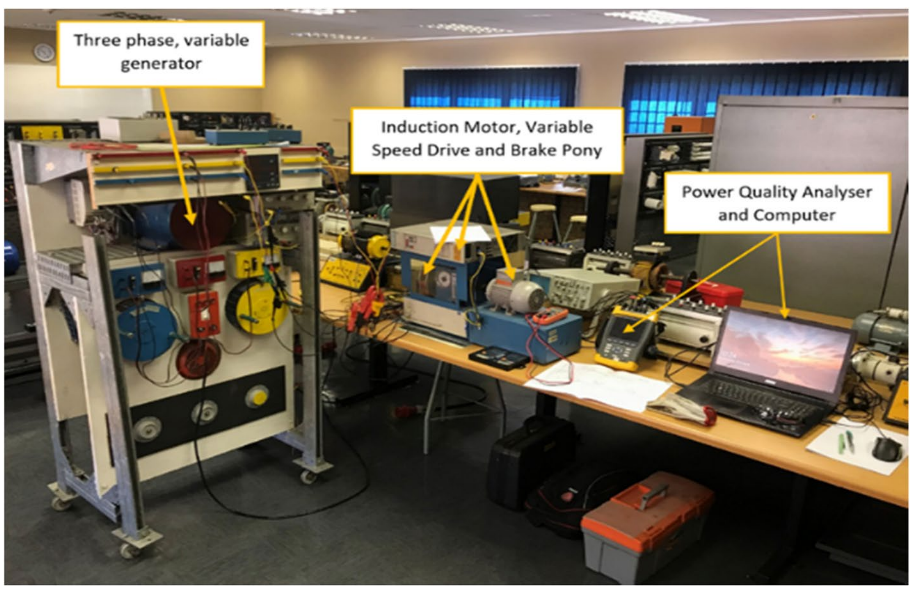

Fig. 2 Showing the experimental test-bench as utilized during the experiments

parameters. The statistical analysis method used in this work involves the inference statistical method, which was basically aimed at characterizing the harmonics generated by an adjustable speed driven induction motor system when subjected to a complex voltage unbalanced supply. This includes the formulation of mathematical model of induction motor system that is being driven by VSD supplied with complex voltage unbalance supply conditions. The mathematical model is then simulated with the aid of MATLAB Simulink. The simulation provides a basis for analysis and characterization of harmonics generated by an adjustable speed driven induction motor system when subjected to a complex voltage unbalanced supply. For validation, an experimental investigation is performed to clearly demonstrate and compare the effects of VSD generated harmonics on a VSD driven induction motor system being subjected to complex voltage unbalances.

Model mathematical derivation

In an investigation titled, “Effects of voltage supply unbalance on AC harmonic current components produced by AC/DC converters” the authors presented a method for modelling and analyzing harmonic and inter-harmonic currents produced from the VSD of the VSI fed pulse-width modulation (PWM) [14]. In the presentation, THD and an analysis of harmonic spectra are represented based on an iterative method that uses the principle of modulation analytical model. The prediction of the characteristic inter-harmonics produced is based on the following equations:

$$f_{Ih} = (6p \pm 1)f_s \pm kf_1 \tag{1}$$

With the DC link dominant harmonics, propagating to the supply side according to

$$f_s = (6p \pm 1)f_s \tag{2}$$

where

p is the pulse

An interesting point of note is that Eq. (1) is often used to calculate the expected multiples of spectra being produced in varying degrees of correction constantly added.

In the paper titled; "Accurate assessment of harmonic and inter-harmonic currents generated by VSI-fed drives under unbalanced supply voltages", the authors presented a balanced rectifier and inverter topology for supply imbalances [21]. However, other authors investigated 6-pulse uncontrolled rectifier with regulated inverter topology in [22]. Here, the authors quantify the harmonic generation observed according to current indices, i.e., THDi and total harmonic distortion from voltage difference (THDv). Spectrum analysis of this investigation suggests a correlated outcome between 5 and 7th harmonic current peaks simulated and experimentally obtained to an average of 55% and 37% for both multiples.

$$\left|2f_{out} \pm f_{in}\right| \tag{3}$$

$$f(t) = \frac{MV}{2}cos(\omega_s t) + \frac{2V}{\pi}\sum_{m=1}^{\infty} J_0\left(mM\left(\frac{\pi}{2}\right)sin\left(m\left(\frac{\pi}{2}\right)\right)cos(m\omega_c t)\right)$$

$$+\left(\frac{2V_d}{\pi}\right)\sum\nolimits_{m=1}^{\infty}\sum\nolimits_{n=\pm 1}^{\pm\infty}\left(\frac{\mathrm{J_n}\left(\mathrm{mM}\left(\frac{\pi}{2}\right)\right)}{\mathrm{m}}\right)\sin\left(\mathrm{m}+\mathrm{n}\left(\frac{\pi}{2}\right)\right)\cos\left(\mathrm{m}\omega_\mathrm{c}+\mathrm{n}\omega_\mathrm{s}\mathrm{t}\right) \tag{4}$$

where

’ω_c = frequency of carrier wave

’ω_s = frequency of modulator wave

’M = modulating index

’m, n = integer numbers

’V_d = DC voltage magnitude

’J_0, J_n = Bessel functions of the first order

The DC link current equations:

$$i_{dc} = \sum_n \sum_m q\left(\frac{VA_n}{Z_n}\right) A_m e^{js`q\theta} e^{-j\pi s`(q-1)} \tag{5}$$

where,

'q = inverter legs

'V = DC link average voltage

'A_n = peak amplitude of the nth harmonic of the phase voltage generated by the inverter

'Z_n = impedance of the nth harmonic between the output terminal of the kth inverter leg and the midpoint of the DC supply

'A_m = peak amplitude of the mth harmonic of switching function

$$V_d i_d = \sum_u v_{uo} \times i_u \tag{6}$$

With:

'u = A, B, C'

To facilitate the measured conduction time for the inverter and rectifier sub parts, the simplified equations for the DC relation voltage and current are realized by the use of switching and transfer functions. In order to promote a stepped switching function output relative to the width output function, PWM is used for the exact conduction time to

$$S_{AN} = \frac{M}{2} sin(\omega_I t) + \frac{2}{\pi} J_0 \sum_{m=1}^{\infty} \left(mM\left(\frac{\pi}{2}\right) sin\left(m\left(\frac{\pi}{2}\right)\right) sin(m\omega_c t)\right) + \left(\frac{2}{\pi}\right) \sum_{m=1}^{\infty} \sum_{n=\pm 1}^{\pm\infty} \left(\frac{J_n\left(mM\left(\frac{\pi}{2}\right)\right)}{m}\right) sin\left(m + n\left(\frac{\pi}{2}\right)\right) sin(m\omega_c + n\omega_s t) \tag{7}$$

where

'S_{AN} = phase A switching function'

'J_0, J_n = Bessel function of first kind'

'ω_I = frequency of modulator wave'

'ω_c = frequency of carrier wave'

The National Equipment Manufacturer's Association (NEMA) defines a voltage unbalance as the line voltage unbalance rate (LVUR) as shown in the equation below.

$$\%LVUR = \frac{\text{Max voltage from averageline voltage}}{\text{Average line voltage}} \times 100 \tag{8}$$

The generalized DC connection voltage equations and the National Environmental Management Act (NEMA) mathematical description do not take the phase angles into account, but only the values of the line voltage.

Similarly, the IEEE's description, only takes into account the phase voltages and not the phase angles of the complex quantities as shown in Eqs. (9, 10, 11 and 12).

$$\%PVUR = \frac{\text{Max voltage from average phase voltage}}{\text{Average phase voltage}} \times 10 \tag{9}$$

The true definition of a voltage unbalance takes into account the magnitude and the phase angle as the mathematical voltage value is complex in nature, as shown below in the equations.

$$\%\text{VUF} = \frac{\text{Negative sequence voltage component}}{\text{Positive sequence voltage component}} \times 100 \tag{10}$$

$$V_{\text{Positive sequence component}} = \frac{V_{ab} + aV_{bc} + a^2V_{ca}}{3} \tag{11}$$

$$V_{\text{Negative sequence component}} = \frac{V_{ab} + a^2V_{bc} + aV_{ca}}{3} \tag{12}$$

Variable speed drive

To facilitate the conduction time of the inverter section, the model uses switching functions and transfer functions suggested in [16], while the rectifier section is modelled according to Park Transform that also makes use of switching functions to facilitate the duration of conduction. A harmonic component can be described as an order component greater than one of a periodic quantity of a Fourier series. This description shows that harmonics on voltage and current wave types are simply distortions. With resonant circuit operation, which supports harmonic propagation through VSD subsystems, significant multiplication of harmonics is present.

Rectification section

To promote the conduction cycle needed to convert the AC to DC, the rectifier utilizes a non-switching model. This is facilitated by the transformation of the input phase voltages by the Park Transform, which is then activated by the switching mechanism to facilitate the conversion for the duration of the necessary conduction.

Triple harmonics produced are directly proportional to the supply side unbalance applied where an amplified magnitude would result in the oscillation of the magnitude of each harmonic multiple. For both cumulative and destructive analysis, this argument supports propagation transfer theory and wave-based analysis, per sub-system in the analysis and subsequent quantification and classification [17, 20]. Triple harmonics are also prevalent under conditions of supply unbalance.

In relation to the action of commutation, controlled versus uncontrolled rectifier interaction is directly proportional to the actual harmonics produced, either forced for controlled or gated applications or naturally commutated. The significance of this is that the conductive duration regulation by the PWM directly affects the harmonic and inter-harmonic distortion generated by controlling the oscillation of each phase from AC to DC or vice versa.

The output voltage and current equations are as follows:

$$V_{dq0} = (\text{Switching Function})^T V_{abc} = \frac{3\sqrt{3}}{\pi}\sqrt{V_d^2 + V_q^2} \tag{13}$$

$$I_{abc} = \left(\text{Switching Function}\right) I_d \tag{14}$$

The switching function is

$$T = \begin{bmatrix} Cos(\omega t) & Cos(\omega t - 120°) & Cos(\omega t + 120°) \\ -Sin(\omega t) & -Sin(\omega t - 120°) & -Sin(\omega t + 120°) \end{bmatrix} \tag{15}$$

Induction motor

For exact parameters that dynamically relates rotor and stator variables flux linkage equations, a dynamic direct (d) to quadrature (q) transformation is utilized.

Experimental setup

As shown in Fig. 2, a three-phase complex variable supply, VSD, Induction Motor (IM) and pony-brake, along with a Fluke power quality analyser (PQA) and laptop, are part of the experimental setup. Through the direct USB connection between the device and the PQA, data collection is facilitated. The findings are catalogued per experimental run.

Simulation

A high-level framework of MATLAB® Simulink model developed, with sub-system designations assigned to each sub-system, is shown in Fig. 3.

Figure 4 depicts the rectification section of the model, related to Eqs. (4), (5), and (6), as implemented in the final Simulink MATLAB model.

Figure 5 depicts the DC link and Inverter sections of the model, related to Eqs. (7) through to (15) with additional MATLAB output and measurement models, as implemented in the final Simulink MATLAB model.

Figure 6 depicts the high-level layout of the induction motor, as implemented in the final Simulink MATLAB® model. The modelling and simulation of an induction motor system powered by VSD was completed with the simulation results, interpreted, and compared with other distortions. A general observation indicates that in the rectification unit of the model, the generation of zero sequence sections or triple harmonic losses, the output-controlled inverter provides a more stable output compared to the VSD input. Through the harmonic multiples observed, the stable average generation of harmonics is noted, suggesting a stable transient behaviour of the model.

Results and discussion

The results for each manufacturer of OEM are shown in Fig. 7 with a significant increase in THD observed in OEM 2. In addition, between the multiples, the harmonic multiples created for each OEM, 2nd through to 9th, were averaged.

The THD refers to total average loss and many measures are used to quantify harmonic content or contamination in a device.

Further considering the harmonic multiples generated for each OEM, 2nd through to 9th, averaged between the multiples. The notable magnitude difference between VSD

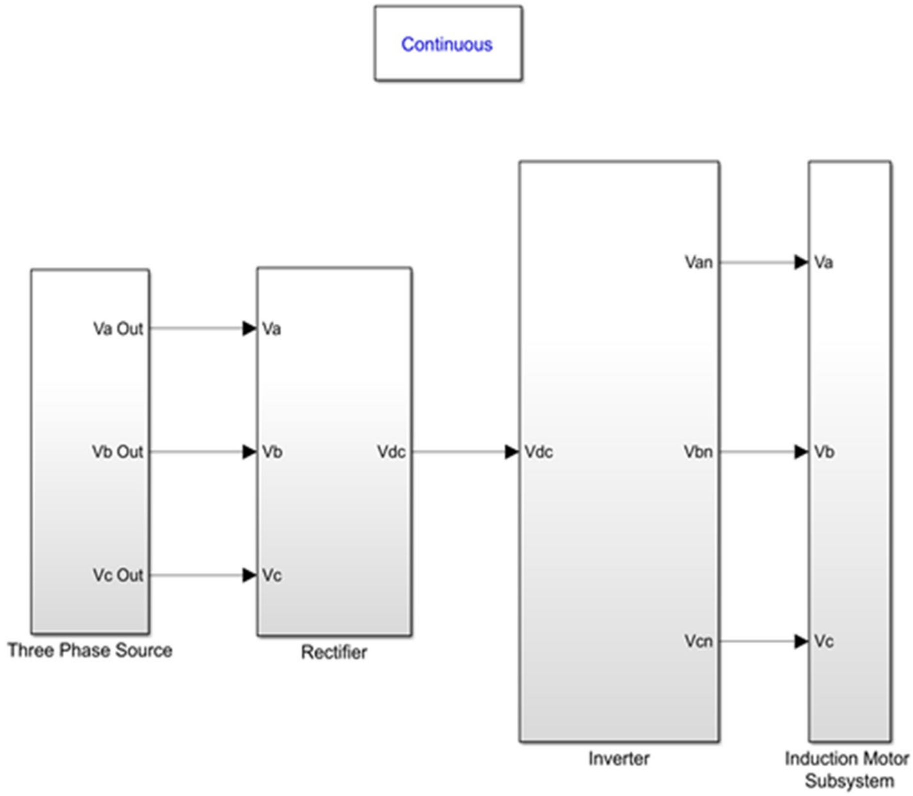

Fig. 3 The high-level model in Simulink

input versus output is clear, with a similar observation for the simulated results obtained. A similar trend progression is observed with both VSD input and output for THD. As shown in Fig. 8, the lack of 4th, 5th, and 6th harmonic multiples is perplexing, as the presence of the 3rd and 9th triple components are present but the 6th multiple not being generated. The naturally expected step degradation with regard to harmonic multiples is not observed on the three OEM's performance, which is also perplexing.

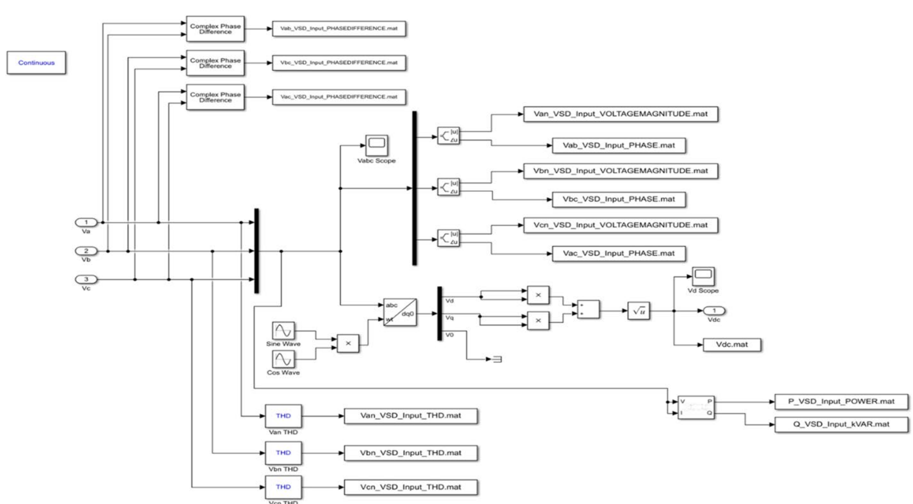

Fig. 4 Components of the rectifier block

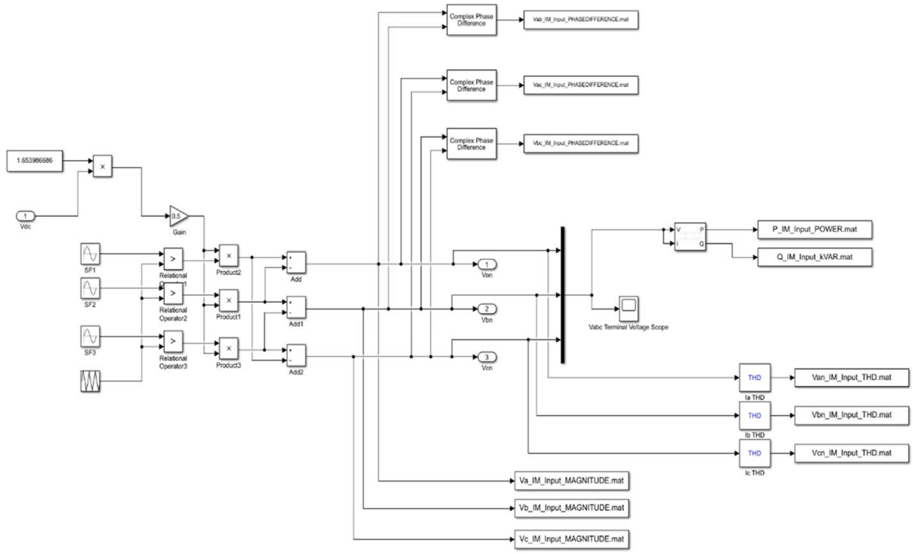

Fig. 5 DC link and inverter

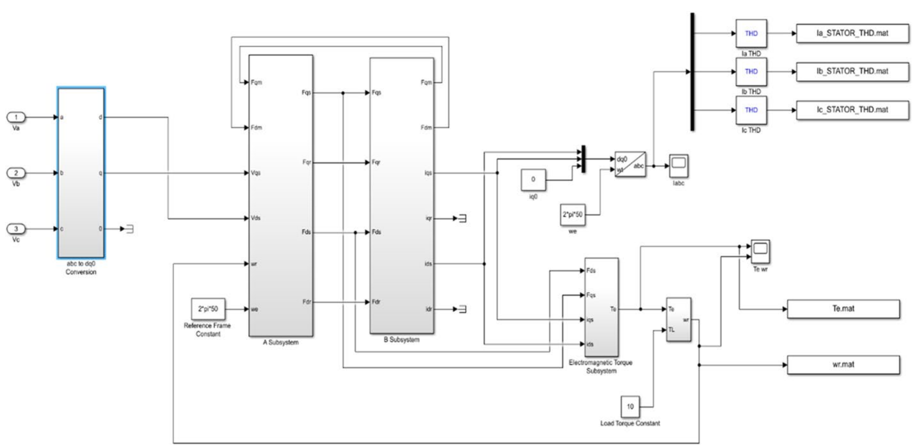

Fig. 6 High-level layout of the induction motor

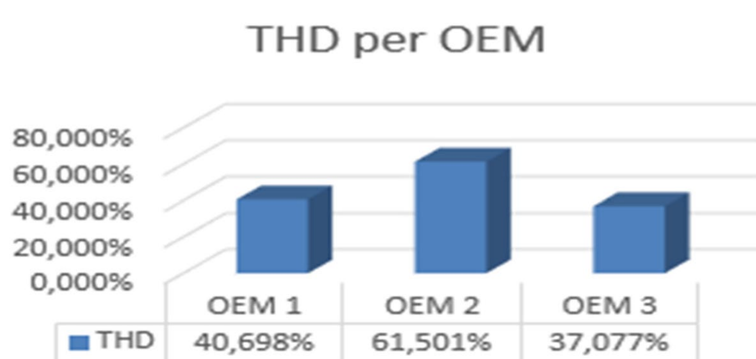

Fig. 7 THD for OEM

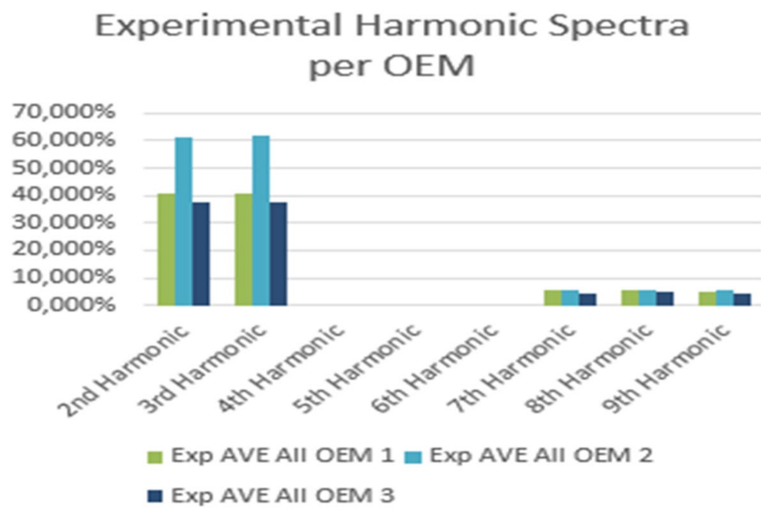

Fig. 8 The harmonic spectra per OEM

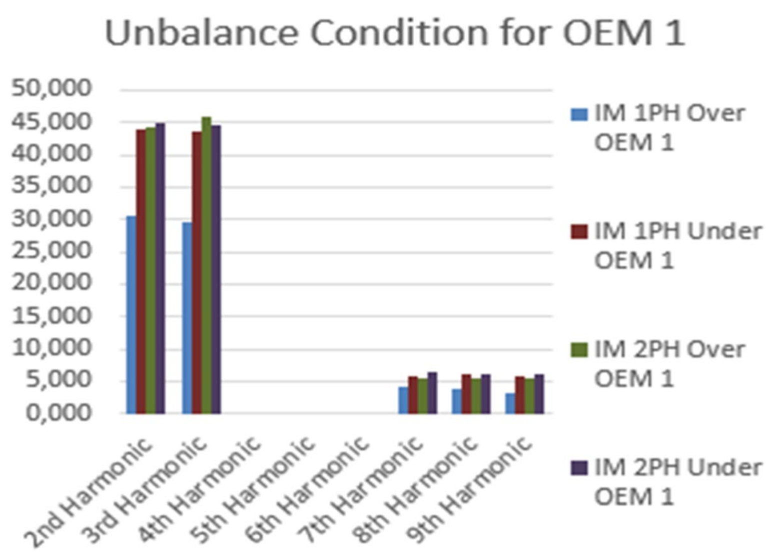

Fig. 9 An unbalance condition for OEM 1

Further considering the per unbalance condition the system was subjected to, for OEM 1 as indicated in Fig. 9.

The harmonic spectrum was summed to an average, per fault condition measure for THD and the produced harmonic spectra for the simulated results, per unbalance condition. The findings as shown in Fig. 10 is first compared with both IM input and VSD input. In the 5th, 8th harmonic multiple and THD, the only correlation is observed between the two parts of the system, with the rest of the harmonic multiples suggesting a major difference in the losses produced in the system. Notably, the results obtained for the IM with the average high zero sequence components recorded for the 3rd, 6th, and 9th harmonic multiples indicate the existence of zero sequence components, resulting in excessive heat generation in the components of the motor, which is a function of the simulated imbalance conditions.

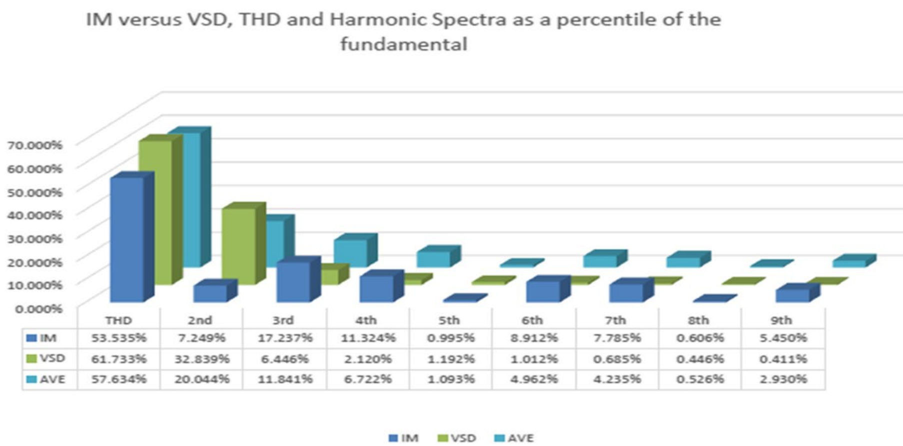

Fig. 10 IM versus VSD, per measuring point, THD and harmonic spectra, as a percentile of the fundamental

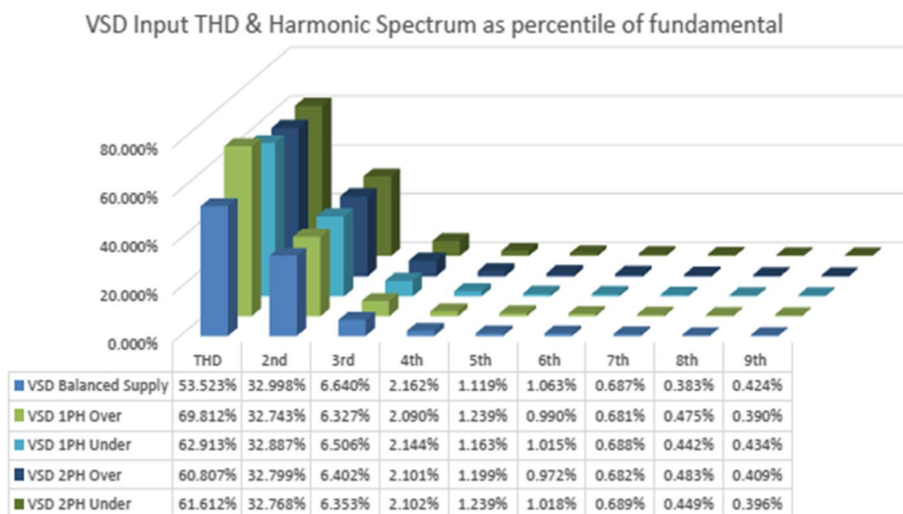

Fig. 11 VSD input THD and harmonic spectrum as percentile of fundamental

The single (1) phase over-voltage unbalance condition is observed as deviating from the average based on the summary performance per simulated unbalance condition. Delving into the particular unbalance state, the findings per measurement point are shown in Fig. 11.

The loss in THD is high, with an estimated magnitude of about < 17.00%, totaling 61.08%. For harmonic multiples, 4th and 7th positive sequence component losses are noted, with average magnitudes observed as predicted at magnitudes of about < 20.00%. For harmonic multiples 2nd, 5th, and 8th, negative sequence portion losses are observed with average magnitudes observed as predicted at < 12.00%, < 1.00%, and < 1.00% respectively per multiple. With predicted magnitudes, high triple multiple magnitudes are observed as < 9.00% and actuals are noted as shown in Fig. 12. The high losses observed demonstrate the instability with regard to producing losses of the uncontrolled 6-pulse rectifier.

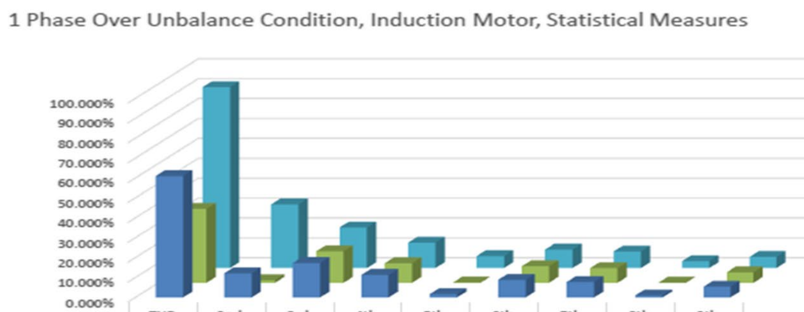

	THD	2nd	3rd	4th	5th	6th	7th	8th	9th
Simulation Run # IM 1PH Over	61.081%	12.2063%	17.3421%	11.3449%	1.7204%	8.9068%	7.8027%	1.0291%	5.4425%
MIN IM 1PH Over	37.154%	1.327%	15.810%	9.813%	0.191%	8.300%	7.395%	0.113%	5.240%
MAX IM 1PH Over	90.910%	31.945%	20.382%	12.781%	5.980%	9.275%	8.304%	3.493%	5.570%

Fig. 12 One phase over unbalance condition

Under this unbalance test, the stable variable velocity drive input measuring point of harmonic loss generation is far below the predicted measurement margins, suggesting that the generation of 6-pulse uncontrolled rectifier losses is negligible. Similarly, in order to determine the cause of the high THD measure, implies that an unbalanced condition study must be carried out on the individual measures. Based on the results obtained, the experimental work showed successful validation. These findings were further evaluated, compared, and discussed with general observations noted in the instances. Furthermore, the experimental results showed an inversion of the active source of harmonic generation from the rectifier to the inverter as compared to the simulation results. This phenomenon is due to high conditions of unbalance, denoted by the high percentiles of VUF and natural resonance occurring through the experimental test work at the VSD output. All the OEM hardware have static low-harmonic filters mounted as usual, but with no denoted specification. This impact is observed in the natural decay of the harmonic multiples, at a rate of increase compared to the simulated performance. This suggests that in variable speed drive implementations in the industry, mitigation techniques have been made traditional.

Conclusions

A consistency between simulated results and experimental results confirmed effective modelling of VSI from VSD. Observations made on the entire system show effects and causes of the harmonics with which the produced harmonics were characterized under different conditions. A clearer insight was given on device subjected to various unbalance conditions in a semi-isolated system in terms of loss generation via the method proposed in this study, to provide understanding of the effect of harmonics and associated losses which often needs to be treated carefully as related to variable speed induction motor.

The experimental results confirmed that unregulated 6-pulse converter produced on average more harmonics compared to regulated converter, as well as that of the standard recommended guideline as to permissible harmonic tolerance. Effective statistical tool when correctively use with some developed electrical model can be effectively used to investigate and reduce the effect of harmonics as shown in this study. However, no connection between the power quality indices used shows that any indicative relationship could be drawn. Further research is required to develop the complex variable supply generator to be automated such that, fine-tuning adjustments can be facilitated, to supply voltage magnitudes and phase displacements as generated. Additionally, investigation of different PWM techniques, and topologies, subjected to complex voltage unbalances, such that a full de-ration spectrum could be compiled. Analyses of this compilation may be utilized to develop a de-ration system for VSD implementations in the industry. Consequently, comparison of the developed dynamic model performance relative to international standard IEC 60,034–1 can be completed to determine in detail, the comparative performance of the induction motor model.

Abbreviations

VSD	Variable speed drive
OEM	Original equipment manufacturer
THD	Total harmonic distortion V
VSI	Voltage source inverter
CSI	Current source inverter
CCM	Continuous current mode
DCM	Discontinuous current mode

Acknowledgements
We would like to acknowledge Tshwane University of Technology for providing all necessary equipment required for the practical set up.

Authors' contributions
D. E. Okojie contributed to the study idea, design, analysis, and also provided scientific content to the manuscript preparation and revision. H. O. Omoregbee drafted/prepared the paper and made revisions to submission of the manuscript. C. G. Richards is an advisor and gave access to essential research materials. A. F. Nnachi is an advisor, contributed to the experimental design, setup, and simulation. B. W. Bornebroek contributed to the conception, data collection, and experimental design. However, all authors reviewed the results and approved the final version of the manuscript.

Funding
This study received no funding from any source.

Availability of data and materials
The datasets generated during and/or analyzed during the current study are available from the corresponding author on reasonable request.

Declarations

Competing interests
The authors declare that they have no competing interests.

Received: 1 January 2022 Accepted: 21 September 2022
Published online: 23 October 2022

References

1. Singh GK (2009) 'Power system harmonics research: a survey', European Transactions on Electrical Power. Euro Trans Electr Power 19:151–172. https://doi.org/10.1002/etep.201
2. Amrei SRH, Xu DG, Lang YQ (2005) 'Harmonics and Inter-harmonics in General VSI/CSI Inverters: Analysis, Modeling and Simulation', IEEE International Conference on Industrial Technology. Piscataway, IEEE, Hong Kong, p 75–80. https://doi.org/10.1109/ICIT.2005.1600613
3. Basic D (2010) Input current inter-harmonics of variable-speed drives due to motor current imbalance. IEEE Trans Power Delivery 25(4):2797–2806. https://doi.org/10.1109/TPWR.2010.2044811
4. Snehal R, Dnyaneshwar D (2016) A review of harmonics detection and measurement in power system. Int J Comput Appl 143(10):42–45. https://doi.org/10.5120/ijca2016910394
5. Ogunyemi O (2019) Power system harmonics. JETP 9(3):8–19. https://doi.org/10.7176/JETP
6. Tabora JM, Tostes ME, De Matos EO, Bezerra UH, Soares TM, De Albuquerque BS (2020) Assessing Voltage Unbalance Conditions in IE2, IE3 and IE4 Classes Induction Motors. IEEE Access 8:186725–186739. https://doi.org/10.1109/access.2020.3029794
7. South African National Standard (1816:2019), Electricity Supply – Quality of supply: Power quality monitoring instruments specification. https://www.gov.za/sites/default/files/gcis_document/201911/42812gen593.pdf
8. South African National Standard (62586:2018) Power quality measurement in power supply systems - Part 1 & Part 2. https://www.google.com/url?sa=t&rct=j&q=&esrc=s&source=web&cd=&cad=rja&uact=8&ved=2ahUKEwjBz_

Lc57z6AhXLTMAKHYT_DNs4ChAWegQIBRAB&url=https%3A%2F%2Fstore.sabs.co.za%2Fcatalog%2Fproduct%2Fview%62586-2-ed-1-00-1%2F&usg=AOvVaw0G5YztpIlrB0nvVop6Sf-Q
9. IEEE 6th International Power Electronics and Motion Control Conference (IPEMC) Wuhan, China 17-20 May 2009. Wuhan, 5/17/2009 - 5/20/2009. IEEE, Piscataway NJ, 2009. pp. 2464–2467. https://www.tib.eu/en/suchen/id/TIBKAT:608911658/
10. Xu WW (1992) A practical harmonic guideline for adjustable speed drive applications. IEEE Trans Power Delivery 7(1):427–433. https://doi.org/10.1109/61.108937
11. Moradi A, Yaghoobi J, Alduraibi A, Zare F, Kumar D, Sharma R (2021) Modelling and prediction of current harmonics generated by power converters in distribution networks. IET Gener Transm Distrib 15(15):2191–2202. https://doi.org/10.1049/gtd2.12166
12 Phukon LJ, Baruah N (2015) A Generalized Matlab Simulink Model of a Three Phase Induction Motor. IJIRSET 4(5):2926–2934. https://doi.org/10.15680/IJIRSET.2015.0405036
13. Sutherland PE (2014) 'Harmonics in electrical power systems: Effects of new technologies', IEEE Industry Applications Society annual meeting. Vancouver, BC. Vancouver, BC, 10/5/2014 - 10/9/2014. IEEE, Piscataway, NJ, p 1–13. https://doi.org/10.1109/IAS.2014.6978493
14. Kumar KV, Michael PA, John JP, Kumar SS (2010) Simulation and comparison of SPWM and SVPWM control for three phase inverter. ARPN (JEAS) 5(7):61–74
15. Chang GW, Chen SK (2004) 'Characterizing harmonic and inter-harmonic currents generated by the VSI-fed adjustable speed drives', International conference on power system technology: POWERCON. IEEE, Singapore, p 475–480. https://doi.org/10.1109/ICPST.2004.1460041
16. Xie X, Liu JCP, Poon FNK, Pong MH (2001) 'Current-Driven Synchronous Rectification Technique for Flyback Topology'. IEEE 32nd Annual Power Electronics Specialists Conference (IEEE Cat. No.01CH37230). https://doi.org/10.1109/PESC.2001.954044
17. Sinvula R, Ez KMA-A, Kahn MT (2020) A Proposed Harmonic Monitoring System for Large Power Users Considering Harmonic Limits. Energies 13:4507. https://doi.org/10.3390/en13174507
18. Rane M, Wagh S (2019) Mitigation of harmonics and unbalanced source voltage condition in standalone microgrid: positive sequence component and dynamic phasor based compensator with real-time approach. Heliyon 5:e01178. https://doi.org/10.1016/j.heliyon.2019.e01178
19. Lodhi E, Wang F-Y, Xiong G, Mallah GA, Javed MY, Tamir TS, Gao DW (2021) A dragonfly optimization algorithm for extracting maximum power of grid-interfaced PV systems. Sustainability 13:778. https://doi.org/10.3390/su131910778
20. Oliveira SEM, Guimaraes JORP (2007) Effects of voltage supply unbalance on AC harmonic current components produced by AC/DC converters. IEEE Trans Power Delivery 22(4):2498–2507. https://doi.org/10.1109/TPWRD.2007.905546
21. Chang GW, Chen SK, Su HJ, Wang PK (2011) Accurate assessment of harmonic and inter-harmonic currents generated by VSI-fed drives under unbalanced supply voltages. IEEE Trans Power Delivery 26(2):1083–1091. https://doi.org/10.1109/TPWRD.2010.2089473
22. Uma D, Vijayarekha K (2017) Modeling and simulation of VSI fed induction motor drive in Matlab/Simulink. IJECE 7(2):584–595. https://doi.org/10.11591/ijece.v7i2

Publisher's Note

Springer Nature remains neutral with regard to jurisdictional claims in published maps and institutional affiliations.